Langmuir

Article

pubs.acs.org/Langmuir

pH and Reduction Dual-Bioresponsive Polymersomes for Efficient Intracellular Protein Delivery

Jinchao Zhang,[†] Liangliang Wu,[†] Fenghua Meng,[†] Zhongjuan Wang,[‡] Chao Deng,[†] Haiyan Liu,[‡] and Zhiyuan Zhong*[,†]

[†]Biomedical Polymers Laboratory and Jiangsu Key Laboratory of Advanced Functional Polymer Design and Application, Department of Polymer Science and Engineering, College of Chemistry, Chemical Engineering and Materials Science, Soochow University, Suzhou, 215123, P. R. China.

[‡]Laboratory of Cellular and Molecular Tumor Immunology, Institute of Biology and Medical Sciences, Soochow University, Suzhou 215123, P. R. China

Supporting Information

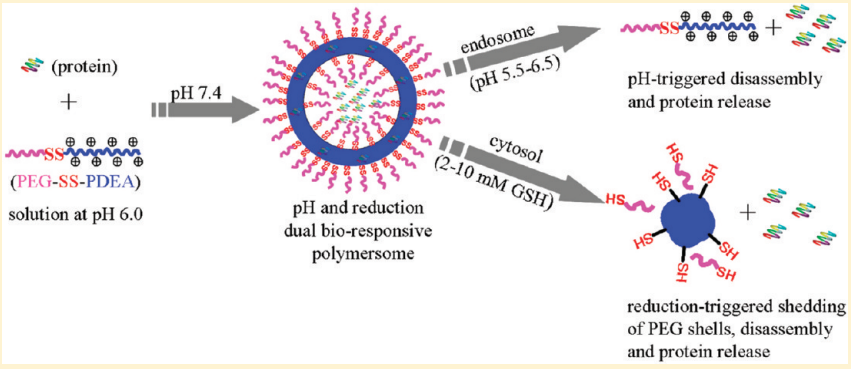

ABSTRACT: pH and reduction dual-bioresponsive nanosized polymersomes based on poly(ethylene glycol)-SS-poly(2-(diethyl amino)ethyl methacrylate) (PEG-SS-PDEA) diblock copolymers were developed for efficient encapsulation and triggered intracellular release of proteins. PEG-SS-PDEA copolymers with PDEA-block molecular weights ranging from 4.7, 6.8, to 9.2 kg/mol were synthesized in a controlled manner via reversible addition−fragmentation chain transfer (RAFT) polymerization of 2-(diethyl amino)ethyl methacrylate (DEAEMA) using PEG-SS-CPADN (CPADN = 4-cyanopentanoic acid dithionaphthalenoate; M_n PEG = 1.9 kg/mol) as a macro-RAFT agent. These copolymers existed as unimers in water at mildly acidic pH (<7.2) conditions, but readily formed monodisperse nanosized polymersomes (54.5−66.8 nm) when adjusting solution pH to 7.4. These polymersomes were highly sensitive to intracellular pH and reductive environments, which resulted in fast dissociation and aggregation of polymersomes, respectively. Notably, both fluorescein isothiocyanate (FITC)-labeled bovine serum albumin (FITC-BSA) and cytochrome C (FITC-CC) proteins could facilely be encapsulated into polymersomes with excellent protein-loading efficiencies, likely as a result of electrostatic interactions between proteins and PDEA. The in vitro release studies showed that protein release was minimal (<20% in 8 h) at pH 7.4 and 37 °C. The release of proteins was significantly enhanced at pH 6.0 due to collapse of polymersomes. Notably, the fastest protein release was observed under intracellular-mimicking reductive environments (10 mM dithiothreitol, pH 7.4). MTT assays in RAW 264.7 and MCF-7 cells indicated that PEG-SS-PDEA (9.2 k) polymersomes had low cytotoxicity up to a polymer concentration of 300 μg/mL. Confocal laser scanning microscope (CLSM) observations revealed that FITC-CC-loaded PEG-SS-PDEA (9.2 k) polymersomes efficiently delivered and released proteins into MCF-7 cells following 6 h of incubation. Importantly, flow cytometry assays showed that CC-loaded PEG-SS-PDEA (9.2 k) polymersomes induced markedly enhanced apoptosis of MCF-7 cells as compared to free CC and CC-loaded PEG−PDEA (8.9 k) polymersomes (reduction-insensitive control). These dual-bioresponsive polymersomes have appeared to be highly promising for intracellular delivery of protein drugs.

INTRODUCTION

In the past decades, protein and peptide-based biopharmaceutics have attracted widespread interest for the effective treatments of various human diseases including diabetes and cancers.[1−3] As compared to small molecule chemical drugs, biopharmaceutics usually exhibit high specificity and therapeutic activity. Notably, many protein therapeutics such as

Special Issue: Bioinspired Assemblies and Interfaces

Received: September 30, 2011
Revised: November 22, 2011
Published: December 21, 2011

Scheme 1. Illustration of pH and Reduction Dual-Bioresponsive Polymersomes Based on PEG-SS-PDEA Diblock Copolymer for Facile Loading and Triggered Intracellular Release of Proteins

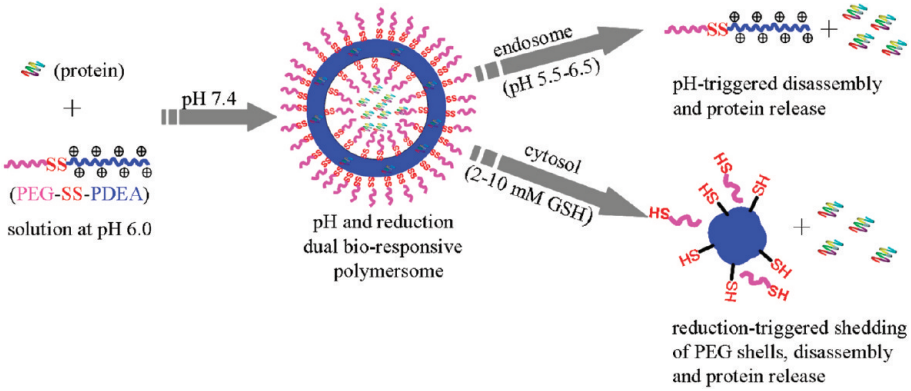

cytochrome C (CC), BAX, and caspase-3 only take effect in specific intracellular compartments such as cytoplasm.[4,5] However, protein drugs often encounter issues of rapid degradation following injection, potential immune response, inferior cellular uptake, and poor intracellular trafficking. In the past years, various types of nanovehicles[6] such as liposomes,[7] polyion complex micelles,[8] nano- and microparticles,[9,10] and nanocapsules[11] have been explored for intracellular protein delivery. These delivery approaches, nevertheless, require use of organic solvents possibly leading to protein denaturation, involve chemical modification of proteins, have low protein loading, and/or display slow and inadequate protein release inside cells.

In recent years, polymersomes with large aqueous compartments as well as robust hydrophobic membranes have emerged as one of the most ideal nanocarriers for encapsulation and controlled delivery of water-soluble proteins and peptides.[12−15] In contrast to liposomes, most polymersomes are intrinsically stealthy since they are typically made from amphiphilic copolymers based on nonfouling polymers such as poly(ethylene glycol) (PEG) and dextran. Varying types of proteins could be loaded into the aqueous lumen and/or the hydrophobic wall of polymersomes.[16,17] For example, Palmer et al. reported that hemoglobin-loaded PEG−poly(ε-caprolactone) (PEG−PCL) polymersomes had similar oxygen affinities to human red blood cells.[18] Discher et al. explored encapsulation of insulin into PEG−polybutadiene (PBD) polymersomes.[12] Kokkoli et al. reported that PR_b (an effective $\alpha_5\beta_1$ targeting peptide)-functionalized poly(ethylene oxide) (PEO)−PBD polymersomes efficiently delivered tumor necrosis factor-α (TNFα) to LNCaP human prostate cancer cells.[19] It should be noted, nevertheless, that polymersomes in general exhibit low protein loading contents and loading efficiencies. We recently reported that biodegradable chimaeric polymersomes based on asymmetric PEG−PCL−PDEA triblock copolymers could efficiently encapsulate exogenous proteins via electrostatic interactions.[20]

To maximize therapeutic outcome, loaded proteins should be released rapidly at the sites of action. In the past several years, different types of stimuli-responsive polymersomes have been developed for programmed drug delivery.[21,22] In particular, pH and reduction are the two most appealing stimuli, as they exist naturally in certain pathological sites and/or intracellular compartments.[23,24] For example, Forster et al. developed pH-sensitive polymersomes from poly(ethylene oxide)-*b*-poly(2-vinylpyridine),[25] Lecommandoux et al. designed pH and temperature dual-responsive polymersomes based on poly[2-(dimethylamino)ethyl methacrylate]-*b*-poly(glutamic acid),[26] and Deming et al. reported synthesis of pH-sensitive polymersomes from polyarginine-*b*-polyleucine.[27] Armes et al. reported pH-sensitive poly(2-(methacryloyloxy) ethyl phosphorylcholine)-*b*-poly(2- (diisopropylamino) ethyl methacrylate) polymersomes for intracellular doxorubicin (DOX) and DNA release.[28,29] Hubbell et al. reported reduction-sensitive PEG-SS-PPS polymersomes.[30] We recently developed reduction and temperature dual-responsive polymersomes based on PEG−PAA−PNIPAM (PAA= polyacrylic acid; PNIPAM = poly(*N*-isopropylacrylamide)) for facile loading and triggered release of fluorescein isothiocyanate (FITC)-dextran.[31]

In this paper, we report on pH and reduction dual-responsive polymersomes based on poly(ethylene glycol)-SS-poly(2-(diethyl amino)ethyl methacrylate) (PEG-SS-PDEA) diblock copolymers for efficient loading of proteins under mild conditions as well as rapid intracellular release of proteins into cancer cells (Scheme 1). These novel dual-bioresponsive polymersomes were designed based on the following considerations: (i) polymersomes are prepared under extremely mild conditions (i.e., increasing solution pH from 5.5 to 7.4 in water), thereby minimizing protein denaturation and inactivation; (ii) PDEA with cationic nature and high buffer capacity at the endosomal pH range may on one hand facilitate efficient encapsulation and stabilization of proteins by electrostatic interactions and on the other hand assist polymersomes escaping from endosomes via the "proton sponge effect";[20,32] and (iii) polymersomes are likely destabilized in the endo/lysosomal compartments as a result of the solubilizing PDEA block as well as in the cytoplasms owing to cleavage of the intervening disulfide bonds, resulting in efficient cytoplasmic delivery of proteins. The formation of PEG-SS-PDEA polymersomes, loading and in vitro release of proteins, as well as the intracellular protein release behavior and cytotoxicity of CC-loaded PEG-SS-PDEA polymersomes were investigated.

EXPERIMENTAL SECTION

Materials. Methoxy PEG (1900, M_n = 1900 g/mol, Fluka) was dried by azeotropic distillation from dry toluene. 2-(Diethyl amino)-ethyl methacrylate (DEAEMA, 99%, Aldrich) was purified by passing though a basic alumina column. Dimethyl sulfoxide (DMSO) and dichloromethane (DCM) were dried under an argon atmosphere by refluxing over $MgSO_4$ and CaH_2, respectively, and distilled prior to use. Toluene and tetrahydrofuran (THF) was dried under an argon atmosphere by refluxing over sodium wire and distilled prior to use. Azobisisobutyronitrile (AIBN, 98%, J&K) was recrystallized twice

dx.doi.org/10.1021/la203843m | *Langmuir* 2012, 28, 2056−2065

from methanol and hexane prior to use. Cystamine dihydrochloride (98%, Alfa Aesar), N-hydroxysuccinimide (NHS, 98%, Alfa Aesar), 4-nitrophenylchloroformate (NPC, 97%, J&K), dicyclohexyl carbodiimide (DCC, 99%, Alfa Aesar), 1,4-dithio-DL-theitol (DTT, 99%, Merck), CC from equine heart (Sigma), bovine serum albumin V fraction (>98%, Roche), pyrene (97%, Fluka), and nile red (99%, Sigma) were used as received. Annexin V-FITC/PI apoptosis detection kit (Keygentec) was used according to the supplier's information. 4-Cyanopentanoic acid dithionaphthalenoate (CPADN) was synthesized according to literature.[33]

Characterization. ^{1}H NMR spectra were recorded on a Unity Inova 400 spectrometer operating at 400 MHz using $CDCl_3$ as solvent. The chemical shifts were calibrated against residual solvent signals of $CDCl_3$. The molecular weight and polydispersity of the copolymers were determined by a Waters 1515 gel permeation chromatograph (GPC) instrument equipped with two linear PLgel columns (500 Å and Mixed-C) following a guard column and a differential refractive-index detector. The measurements were performed using THF as the eluent at a flow rate of 1.0 mL/min at 30 °C and a series of narrow polystyrene standards for the calibration of the columns. The size of polymersomes was determined using dynamic light scattering (DLS) at 25 °C using a Zetasizer Nano-ZS from Malvern Instruments equipped with a 633 nm He−Ne laser using backscattering detection. The ζ potential of the polymersomes was determined with a Zetasizer Nano-ZS from Malvern Instruments. CLSM images were taken on a confocal microscope (TCS SP2). Transmission electron microscopy (TEM) was performed using a Tecnai G220 TEM operated at an accelerating voltage of 120 kV. The samples were prepared by dropping 10 μL of 0.2 mg/mL polymersome suspension on the copper grid followed by staining with phosphotungstic acid (1 wt %).

Synthesis of PEG-SS-CPADN Macro-RAFT Agent. PEG-SS-CPADN macro-RAFT agent was prepared in three steps. First, PEG hydroxyl terminal group was activated with NPC. Briefly, under an argon atmosphere, to a solution of PEG (M_n = 1900 g/mol, 5.0 g, 2.63 mmol) and pyridine (1.07 mL, 13.16 mmol) in toluene/DCM mixture (30 mL/35 mL) at 4 °C was dropwise added to a solution of NPC (2.12 g, 10.53 mmol) in 25 mL of DCM. The reaction mixture was warmed to 30 °C following the addition of pyridine and stirred for 45 h. The reaction mixture was filtered. The filtrate was concentrated with a rotary evaporator. The product was isolated by precipitation in cold diethyl ether, filtration and drying in vacuo for 48 h. Yield: 84.6%. ^{1}H NMR (400 MHz, $CDCl_3$): δ 8.29, 8.27, 7.40, and 7.37 (aromatic protons of NPC), 4.44 (t, $-OCH_2CH_2OC(O)-$), 3.45−3.81 (m, PEG methylene protons), and 3.38 (s, CH_3O-).

Subsequently, PEG−NPC was reacted with cystamine to yield PEG−cystamine (PEG-Cys). Briefly, under an argon atmosphere, to a solution of cystamine dihydrochloride (5.06 g, 22.47 mmol) and triethylamine (4.38 g, 44.94 mmol) in 30 mL of DMSO at room temperature (r.t.) was added dropwise a DMSO solution (20 mL) of PEG−NPC (4.50 g, 2.25 mmol). The reaction was allowed to proceed at 30 °C for 45 h. The solution was filtered. The adduct was isolated by precipitation in cold diethyl ether, filtration, and drying in vacuo for 48 h. The product was redissolved in 40 mL of DCM and extracted three times with 60 mL of saturated NaCl solution. The final product was recovered by precipitation in cold diethyl ether, filtration, and drying in vacuo for 48 h. Yield: 66.3%. ^{1}H NMR (400 MHz, $CDCl_3$): δ 4.23 (t, $OCH_2CH_2OC(O)$), 3.45−3.81 (m, PEG methylene protons), 3.37 (s, CH_3O-), 3.31 (t, $-SSCH_2CH_2NH_2$), and 3.11 (t, $-CH_2CH_2SSCH_2CH_2NH_2$).

Finally, PEG-SS-CPADN was obtained by coupling CPADN to PEG−Cys via carbodiimide chemistry. Briefly, to a solution of CPADN (0.62 g, 1.88 mmol) and NHS (0.23 g, 1.95 mmol) in 100 mL of DCM at 4 °C was dropwise added a DCM solution (20 mL) of DCC (0.93 g, 4.51 mmol). The reaction mixture was stirred at r.t. for 20 h. PEG−Cys (1.50 g, 0.72 mmol) was added, and the reaction was allowed to proceed for 8 h at r.t. The solution was filtered. The product was isolated by precipitation in cold diethyl ether, filtration, and drying in vacuo for 48 h. Yield: 86.2%. ^{1}H NMR (400 MHz, $CDCl_3$): δ 7.48−8.15 (m, aromatic protons of CPADN), 6.81 (s, $-OC(O)NH-$), 5.62 (s, $-C(O)NH-$), 4.23 (t, $-OCH_2CH_2OC(O)NH-$), 3.41−3.85 (m, PEG methylene protons), 3.37 (s, CH_3O-), 2.81 (m, $-NHCH_2CH_2SSCH_2CH_2NH-$), 2.62 (t, $-NHC(O)CH_2CH_2C(CN)-$), 2.41 (t, $-NHC(O)CH_2CH_2C(CN)-$), 1.90 (s, $-NHC(O)CH_2CH_2C(CN)CH_3$).

Synthesis of PEG-SS-PDEA by RAFT Polymerization. To a Schlenk reaction vessel equipped with a magnetic stirrer were charged DEAEMA (3.12 g, 16.84 mmol), AIBN (4.1 mg, 24.9 μmol), PEG-SS-CPADN (0.50 g, 0.24 mmol), and THF (4.0 mL). After 30 min of degassing with argon, the reaction vessel was sealed and immersed in an oil bath thermostatted at 65 °C. The polymerization was allowed to proceed for 48 h. The resulting copolymer was precipitated in cold diethyl ether, filtered, and dried in vacuo for 48 h. The resulting PEG-SS-PDEA copolymers were further purified by redissolving them in deionized water (50 mL, pH 6.0) and ultrafiltration (MWCO 5000). The final product was isolated by lyophilization. Yield: 76.2%. ^{1}H NMR (400 MHz, $CDCl_3$): δ 4.21 (t, $-OCH_2CH_2OC(O)-$), 4.05 (t, $-C(O)OCH_2CH_2-$), 3.48−3.81 (m, PEG methylene protons), 3.37 (s, CH_3O-), 2.70 (t, $-C(O)OCH_2CH_2-$), 2.56 (q, $-CH_2CH_2N(CH_2CH_3)_2$), 1.90 (s, $-CH_2C(CH_3)-$), 1.04 (t, $-CH_2CH_2N(CH_2CH_3)_2$), 0.95 (s, $-CH_2C(CH_3)-$).

Formation of Polymersomes and Critical Aggregation Concentration (CAC). The polymersomes were facilely prepared by adjusting an acidic solution of PEG-SS-PDEA copolymers (pH 2.0, 0.2 mg/mL) to pH 7.4 or above. To obtain good size distributions, solution pH was increased gradually from pH 5.5 to pH 6.5, 7.0, and finally 7.4, allowing equilibrium for 30 min at each pH. The average sizes of polymersomes obtained at different pHs were determined by DLS. The CAC of the polymersomes was evaluated using pyrene as a fluorescence probe. The polymersome concentrations (3 mL in HEPES) varied from 4×10^{-5} to 4×10^{-2} mg/mL, and pyrene concentration was fixed at 0.6 mM. The fluorescence spectra (FLS920) were recorded with an excitation wavelength of 330 nm. The emission fluorescence at 372 and 383 nm were monitored. The CAC was estimated as the cross-point when extrapolating the intensity ratio I_{372}/I_{383} at low and high concentration regions.

CLSM Observations of Polymersomes Loaded with Nile Red and DOX·HCl. In order to verify the vesicular structure, polymersomes were made as described above in the presence of DOX·HCl. After extensive dialysis (MWCO 3500 Da) to remove free DOX·HCl, 5 μL of nile red in acetone was added (final nile red concentration 0.1 μM). The solution was stirred for 3 h at 37 °C to evaporate acetone. CLSM images were taken using a confocal microscope (TCS SP2).

pH and Reduction-Triggered Destabilization of Polymersomes. The change of polymersome sizes in response to mildly acidic or reductive conditions at pH 7.4 was followed by DLS measurements. Briefly, 0.1 M HCl solution was added to PEG-SS-PDEA polymersome dispersions prepared as described above at pH 7.4 to pH 6.5, and then particle sizes were measured by DLS. The reduction-responsive destabilization of polymersomes was studied by treating polymersome dispersions at pH 7.4 for 8 h with 10 mM DTT, and particle sizes were measured by DLS.

Loading of Proteins. Protein-loaded polymersomes were readily prepared by adjusting the pH of PEG-SS-PDEA and protein aqueous solution at pH 5.5 to 7.4 (10 mM HEPES buffer) followed by extensive dialysis (MWCO 500 kDa) to remove free proteins. Briefly, FITC-labeled cytochrome C (CC) or bovine serum albumin (BSA) was added to PEG-SS-PDEA copolymer solutions in deionized (DI) water at pH 5.5 (polymer concentration 0.2 mg/mL) at varying protein/polymer weight ratios (5−20 wt %). The solution pH was adjusted to 7.4 in 10 mM HEPES buffer and stirred for 8 h. Free proteins were removed by dialysis (MWCO 500 kDa) against HEPES buffer (pH 7.4, 10 mM) for 16 h at 25 °C with at least 5 times change of media. The control experiments on free proteins showed that this purification procedure is sufficient to remove unloaded proteins. To determine protein loading content (PLC) and protein loading efficiency (PLE), protein-loaded polymersomes were disrupted by adding 3 times volume of THF, which led to complete release of loaded proteins. The amount of FITC-labeled proteins was determined by fluorescence measurements based on the calibration curve with known concentrations of FITC-labeled proteins in THF/

Scheme 2. Synthesis of PEG-SS-PDEA Diblock Copolymer via RAFT Polymerization Using PEG-SS-CPADN as a Macro-RAFT Agent

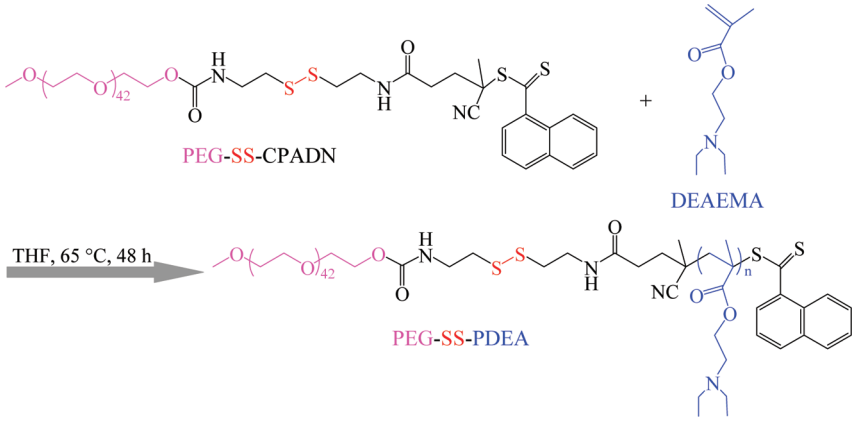

water (3/1, v/v). The calibration curves are shown in Figure S1 (Supporting Information). In case of native proteins, the protein-loaded polymersomes were dialyzed (MWCO 500 kDa) against acetate buffer (pH 6.0, 10 mM, 150 mM NaCl) at 37 °C for 24 h to completely release proteins. The amount of loaded protein was determined by BCA assays according to the supplier's protocols (Thermo Scientific). PLC and PLE were calculated according to the following formula:

$$\text{PLC(wt \%)} = (\text{weight of loaded protein/weight of polymer}) \times 100\%$$

$$\text{PLE(\%)} = (\text{weight of loaded protein/weight of protein in feed}) \times 100\%$$

In Vitro Protein Release. The release of FITC-BSA and FITC-CC from polymersomes was investigated at 37 °C in four different media, i.e., phosphate buffered saline (PBS) buffer (pH 7.4, 20 mM, 150 mM NaCl), PBS buffer with 10 mM DTT, acetate buffer (pH 6.0, 20 mM, 150 mM NaCl), and acetate buffer with 10 mM DTT. Briefly, 1 mL of protein-loaded polymersomes in HEPES buffer (pH 7.4, 10 mM) was dialyzed (MWCO 500 kDa) against 30 mL of the above release media. At desired time intervals, 10 mL of release media was taken out and replenished with an equal volume of fresh media. The amounts of released proteins as well as proteins remaining in the dialysis tube were determined by fluorescence measurements (FLS920, excitation at 492 nm, and emission from 510 to 600 nm). The release experiments were conducted in triplicate, and the results presented are the average data with standard deviations.

MTT Assays. Murine RAW 264.7 macrophages and MCF-7 cells were plated in a 96-well plate (1×10^4 cells/well) using Dulbecco's modified Eagle's medium (DMEM) supplemented with 10% fetal bovine serum, 1% L-glutamine, antibiotics penicillin (100 IU/mL), and streptomycin (100 mg/mL) for 24 h to reach 70% confluency. The cells were then incubated with varying amounts of PEG-SS-PDEA (9.2 k) polymersomes at 37 °C in an atmosphere containing 5% CO_2 for 24 h. Then 3-(4,5-dimethylthiazol-2-yl)-2,5- diphenyltetrazolium bromide (MTT) solution in PBS (5 mg/mL, 10 μL) was added and incubated for another 4 h. The medium was aspirated, the MTT–formazan generated by live cells was dissolved in 150 μL of DMSO, and the absorbance at a wavelength of 490 nm of each well was measured using a microplate reader (Biorad, ELX808 IU). The cell viability (%) was determined by comparing the absorbance at 490 nm with control wells containing only cell culture medium. Data are presented as average ± SD (n = 4).

Flow Cytometry. MCF-7 cells were plated in a 24-well plate (5×10^4 cells/well) under 5% CO_2 atmosphere at 37 °C using DMEM medium supplemented with 10% fetal bovine serum, 1% L-glutamine, antibiotics penicillin (100 IU/mL), and streptomycin (100 μg/mL) for 24 h. The cells were treated with CC-loaded PEG-SS-PDEA (9.2 k) polymersomes, CC-loaded PEG–PDEA (8.9 k) polymersomes (reduction insensitive control), or free CC (CC dosage: 80 μg/mL) for 48 h under 5% CO_2 atmosphere at 37 °C. To quantify apoptotic cells, an Annexin V-FITC kit was used as described by the manufacturer (KenGEN, China). Briefly, MCF-7 cells were digested with EDTA-free trypsin, washed twice with cold PBS, and resuspended in binding buffer at a concentration of 1×10^5 cells/mL. Then, the cells were stained with 5 μL of Annexin V-FITC solution and 5 μL of propidium iodide (PI) solution for 15 min at r.t. in the dark. At the end of incubation, 400 μL of binding buffer was added, and the cells were analyzed immediately using flow cytometry (BD FACSCalibur, Mountain View, CA).

Cellular Uptake and Intracellular Protein Release Studies. MCF-7 cells were plated on microscope slides in a 24-well plate (5×10^4 cells/well) under 5% CO_2 atmosphere at 37 °C using DMEM medium supplemented with 10% fetal bovine serum, 1% L-glutamine, antibiotics penicillin (100 IU/mL), and streptomycin (100 μg/mL) for 24 h. One hundred microliters of FITC-CC-loaded PEG-SS-PDEA (9.2 k) polymersomes, FITC-CC loaded PEG-PDEA (8.9 k) polymersomes, or free FITC-CC (FITC-CC dosage: 40 μg/mL) was added. After incubation at 37 °C for 6 h, the culture medium was removed, and the cells on microscope plates were washed three times with PBS. The cells were fixed with 4% formaldehyde for 20 min and washed 3 times with PBS. The cell nuclei were stained with 4′,6-diamidino-2-phenylindole (DAPI) for 20 min and washed three times with PBS. CLSM images were taken using a confocal microscope (TCS SP2).

RESULTS AND DISCUSSION

Synthesis of PEG-SS-PDEA Block Copolymers. PEG-SS-PDEA block copolymers were synthesized via reversible addition–fragmentation chain transfer (RAFT) polymerization of DEAEMA using PEG-SS-CPADN ($M_{n\,PEG}$ = 1.9 kg/mol) as a macro-RAFT agent (Scheme 2). CPADN is a robust and versatile RAFT agent, with which we have previously prepared PDMA–PCL–PDMA (PDMA = poly(*N*,*N*-dimethylacrylamide), PEG–PCL–PDEA, and PEG–PHEMA (PHEMA = poly(2-hydroxyethyl methacrylate)) block copolymers.[20,34,35] PEG-SS-CPADN was readily obtained with high yield by coupling CPADN to PEG–Cys conjugates via carbodiimide chemistry. ^{1}H NMR showed that the signals at δ 1.90 and 4.21 attributable to the methyl protons of CPADN and the methylene protons of PEG next to the urethane bond, respectively, had an integral ratio close to 3:2, and moreover the signals assignable to the methylene protons next to the primary amino group (δ 3.31) completely disappeared (Figure 1A), indicating quantitative conjugation of CPADN. The RAFT

dx.doi.org/10.1021/la203843m | *Langmuir* 2012, 28, 2056–2065

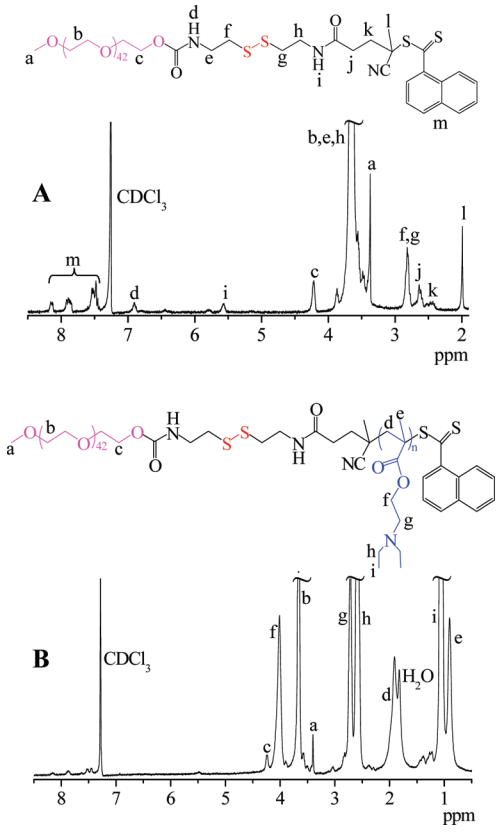

Figure 1. ^{1}H NMR spectra (400 MHz, $CDCl_3$) of PEG-SS-CPADN macro-RAFT agent (A) and PEG-SS-PDEA diblock copolymer (Table 1, Entry 3) (B).

polymerization was carried out in THF at 65 °C for 48 h using AIBN as a radical source. The results of polymerization are summarized in Table 1. ^{1}H NMR displayed that, besides a sharp peak attributable to PEG (δ 3.63), signals characteristic of PDEA block (δ 4.05, 2.70, 2.56, 1.90, 1.04 and 0.95) were also detected (Figure 1B). The molecular weights of PDEA (ranging from 4.7, 6.8, to 9.2 kg/mol) calculated by comparing the integral ratios of signals at δ 4.05 (PDEA methylene protons next to the ester group) and δ 3.63 (PEG methylene protons) increased with increasing DEAEMA/PEG-SS-CPADN mole ratios (Table 1). GPC measurements showed that all copolymers had a unimodal distribution with moderate polydispersity indexes (PDIs) ranging from 1.17 to 1.41 (Table 1). Moreover, the M_n data determined by GPC were close to those obtained by ^{1}H NMR analyses. These combined results indicate that thus prepared PEG-SS-PDEA block copolymers contain a negligible amount of PDEA homopolymers if present. In a similar way, reduction-insensitive PEG–PDEA diblock polymer with an M_n(PDEA) of 8.9 kg/mol and PDI of 1.46 was synthesized using PEG–CPADN as a macro-RAFT agent (Table 1).

Formation of pH and Reduction Dual-Bioresponsive Polymersomes. PEG-SS-PDEA block copolymers were readily soluble in water at pH 2.0–6.5. The DLS measurements showed that these copolymers had average sizes of 7–10 nm at pH 6.5 (Figure 2A), indicating that they exist as a unimer under mildly acidic conditions. However, upon adjusting the solution pH gradually to 7.4, nanoparticles with average sizes varying from 54.5 to 66.8 nm depending on PDEA block lengths and

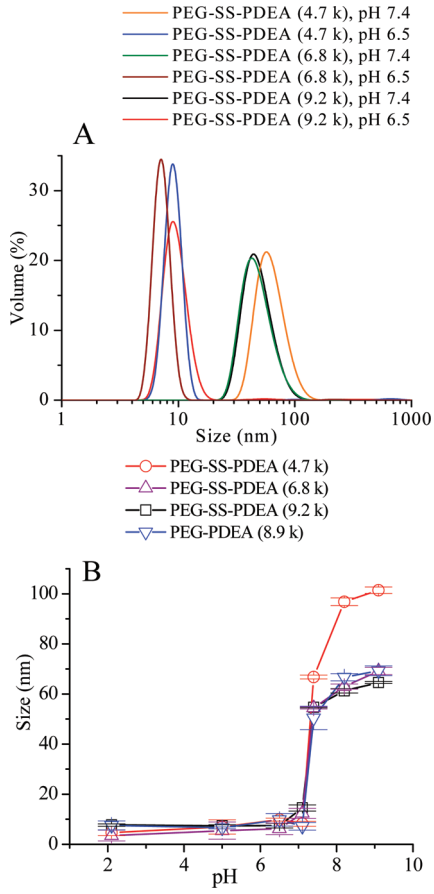

Figure 2. pH-induced formation of nanosized polymersomes from PEG-SS-PDEA and PEG-PDEA diblock copolymers. (A) Size distribution profiles of PEG-SS-PDEA copolymers at pH 6.5 (unimers) and PEG-SS-PDEA polymersomes at pH 7.4. (B) PEG-SS-PDEA and PEG–PDEA diblock copolymer polymersome sizes as a function of pH.

Table 1. Synthesis of PEG-SS-PDEA and PEG-PDEA Diblock Copolymers

		M_n (kg/mol)			M_w/M_n		
entry	copolymer	design	^{1}H NMR[a]	GPC[b]	GPC[b]	size ± SD nm[c]	PDI[c]
1	PEG-SS-PDEA (4.7 k)	1.9–6.0	1.9–4.7	6.3	1.17	66.8 ± 0.8	0.12
2	PEG-SS-PDEA (6.8 k)	1.9–8.0	1.9–6.8	10.7	1.40	54.5 ± 0.4	0.07
3	PEG-SS-PDEA (9.2 k)	1.9–13.0	1.9–9.2	11.7	1.41	54.7 ± 0.2	0.17
4	PEG–PDEA (8.9 k)	1.9–13.3	1.9–8.9	12.9	1.46	50.5 ± 4.6	0.17

[a]Determined by ^{1}H NMR analysis. [b]Determined by GPC (eluent: THF, flow rate: 1.0 mL/min, standards: polystyrene, 30 °C). [c]The average size and size distribution of polymersomes formed at 25 °C and pH 7.4 measured by DLS. The data are presented as mean value ± standard deviation of four independently prepared samples.

dx.doi.org/10.1021/la203843m | Langmuir 2012, 28, 2056–2065

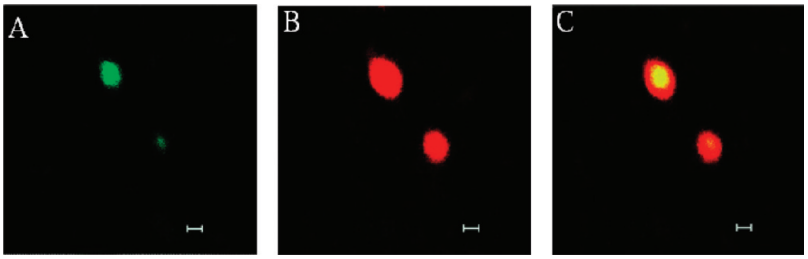

Figure 3. CLSM images of PEG-SS-PDEA (9.2 k) polymersomes loaded with DOX·HCl (hydrophilic) and nile red (hydrophobic). (A) DOX·HCl (green), (B) Nile Red (red), and (C) overlay of images A and B. The scale bar represents 1 μm.

narrow size distributions (PDI 0.07−0.17) were formed due to deprotonation of PDEA block (Figure 2A). Notably, the sizes of nanoparticles highly depended on the rate of neutralization, in which fast increase of pH usually resulted in particles of large sizes as well as broad distributions. The smaller size observed for PEG-SS-PDEA copolymer with higher molecular weight PDEA likely results from its higher hydrophobic weight fraction favoring the formation of high curvatures. PDEA is a weak polybase with a pK_a of ca. 7.2 in water. At pH 7.4 (above its pK_a), PDEA becomes hydrophobic, as its most tertiary amine groups (ca. 70%) are deprotonated. It should be noted that all copolymers exhibited sharp transition at pH 7.2 (Figure 2B), in which the molecular weights of PDEA appeared to have no influence on the transition pH. Above pH 7.4, the nanoparticles grew in size reaching a plateau at pH 8.5−9.0 as a result of deprotonation of the remaining tertiary amine groups of PDEA. It should further be noted that thus formed nanoparticles were sufficiently stable under physiological conditions (pH 7.4, 150 mM NaCl, 37 °C), in which both size and size distribution did not change in 2 days. The unique pH-sensitivity of PDEA has been applied for construction of varying types of pH-responsive micelles as well as polymersomes.[36−38]

These PEG-SS-PDEA block copolymers had low PEG contents of 0.17−0.29 wt.% (Table 1), which favors the formation of vesicular structures.[21,39] TEM confirmed that PEG-SS-PDEA (9.2 k) formed vesicular structures with an average size of ca. 50 nm (Figure S2), close to that determined by DLS. CLSM observations of PEG-SS-PDEA (9.2 k) polymersomes loaded with DOX·HCl (hydrophilic) and Nile Red (hydrophobic) clearly showed colocalization of hydrophilic and hydrophobic molecules. Moreover, The intensity profiles of green and red fluorescence in a captured giant polymersome were in accordance with the location of Nile Red in the membrane and DOX·HCl in the lumen (Figure 3), compliant with their vesicular structure. Adams et al. reported that PEG-*b*-PDEA with 20−30% EG formed 60−80 nm vesicles.[40] The CAC determined using pyrene as a fluorescence probe revealed a low CAC of 8.9, 8.3, and 6.6 mg/L for PEG-SS-PDEA (4.6 k), PEG-SS-PDEA (6.8 k), and PEG-SS-PDEA (9.2 k), respectively, in HEPES (10 mM) at pH 7.4. Notably, these PEG-SS-PDEA polymersomes were stable under physiological salt (150 mM NaCl) conditions.

The pH and reduction-responsive behaviors of thus formed PEG-SS-PDEA polymersomes were investigated using DLS. As expected, PEG-SS-PDEA polymersomes similar to the non-reducible PEG-PDEA polymersomes were rapidly dissociated to unimers when adjusting medium pH to 6.5 (Figure 4A). Interestingly, under a reductive environment containing 10 mM DTT at pH 7.4, PEG-SS-PDEA (9.2 k) polymersomes formed large aggregates of ca. 400 nm in 8 h (Figure 4B). By contrast, no size change was observed for the nonreducible PEG-PDEA

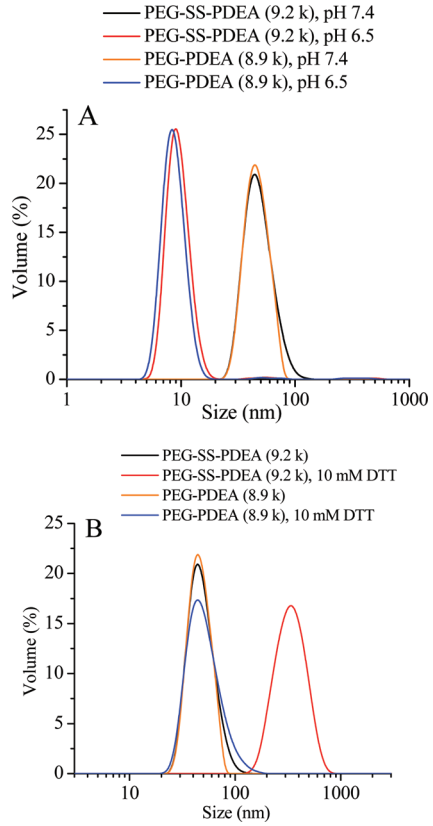

Figure 4. The size changes of PEG-SS-PDEA (9.2 k) and PEG−PDEA (8.9 k) polymersomes in response to pH 6.5 (A) and 10 mM DTT at pH 7.4 for 8 h (B).

(8.9 k) polymersomes under otherwise the same conditions. The aggregation of PEG-SS-PDEA (9.2 k) polymersomes under reductive conditions is most likely due to cleavage of the intervening disulfide bonds, which results in shedding of PEG shells. The effective cleavage of disulfide bond in the presence of 10 mM DTT has been demonstrated for the reduction-responsive shell-sheddable block copolymer micelles.[41,42] It is evident, therefore, that pH and reduction dual-responsive nanosized polymersomes can be facilely prepared from PEG-SS-PDEA block copolymers under mild conditions.

Loading and Triggered Release of Proteins. PEG-SS-PDEA polymersomes were designed herein for active loading and triggered intracellular delivery of proteins. Protein-loaded polymersomes were readily prepared by adjusting the pH of PEG-SS-PDEA and protein aqueous solution at pH 5.5 to 7.4 (10 mM HEPES buffer) followed by extensive dialysis to remove free proteins. We studied the encapsulation and release of two FITC-labeled proteins, BSA and CC. BSA has a low

dx.doi.org/10.1021/la203843m | *Langmuir* 2012, 28, 2056−2065

Table 2. Protein-Loaded PEG-SS-PDEA and PEG-PDEA Polymersomes[a]

copolymer	proteins	theoretical loading content (wt %)	protein loading content (wt %)	protein loading efficiency (%)	size (nm)/PDI	ξ (mV)[b]
PEG-SS-PDEA (9.2 k)	FITC-CC	5.0	5.0	100.0	58.5/0.14	+3.5
		10.0	9.8	97.9	58.6/0.20	+2.4
	FITC-BSA	5.0	4.0	80.6	49.1/0.11	+3.3
PEG-SS-PDEA (6.8 k)	FITC-CC	5.0	4.5	89.9	60.1/0.14	+7.7
		10.0	5.9	58.5	61.2/0.27	+5.6
	FITC-BSA	5.0	4.0	59.9	59.8/0.11	+5.7
PEG−PDEA (8.9 k)	FITC-CC	10.0	9.3	93.3	58.4/0.14	+3.3
	FITC-BSA	5.0	3.8	76.2	61.8/0.16	+2.3

[a]Polymer concentration was set at 0.2 mg/mL in HEPES buffer (pH 7.4). [b]Determined in HEPES buffer (pH 7.4 10 mM).

isoelectric point (pI) of 4.9 while CC has a high pI of 10.2. The results of protein loading are summarized in Table 2. Remarkably, PEG-SS-PDEA (9.2 k) polymersomes exhibited excellent protein loading efficiencies, which were nearly quantitative (97.9−100%) for FITC-CC at theoretical protein loading contents of 5−10 wt % and 80.6% for FITC-BSA at a theoretical protein loading content of 5 wt %. PEG-SS-PDEA (6.8 k) polymersomes revealed in general lower protein loading efficiencies (59.8−61.2%) than PEG-SS-PDEA (9.2 k) polymersomes (Table 2), but their protein loading levels remained high as compared to previously reported protein carriers including liposomes[43] and polymersomes.[44,45] PEG-PDEA (8.9 k) polymersomes, similar to PEG-SS-PDEA (9.2 k) counterparts, also showed superior protein loading levels (Table 2). Notably, the pI of proteins had little influences on the protein loading efficiencies of PEG-SS-PDEA polymersomes, indicating that besides ionic interactions, hydrophobic and/or hydrogen bonding interactions between proteins and PDEA blocks during the polymersome formation might play a significant role in protein encapsulation. In a control experiment, a neutral and hydrophilic large molecule, FITC-labeled 40 kDa dextran, was loaded into PEG-SS-PDEA (9.2 k) polymersomes using the same procedure. Interestingly, a high loading efficiency of 73.1% was also obtained at a theoretical loading content of 5 wt.%. Therefore, the high protein loading level of PEG-SS-PDEA and PEG−PDEA polymersomes is most likely due to the effective electrostatic, hydrophobic, and/or hydrogen bonding interactions between exogenous proteins and PDEA blocks during the polymersome formation as well as to the large aqueous interior of polymersomes.[20]

The average sizes of protein-loaded PEG-SS-PDEA polymersomes varied from 49.1 to 61.2 nm in HEPES buffer (10 mM, pH 7.4) at 37 °C (Table 2), which was similar to the parent empty polymersomes. Notably, these protein-loaded polymersomes maintained low PDIs of 0.11−0.22 (Table 2). The little or no change of polymersome sizes is likely due to the fact that the presence of proteins had essentially no influences on the pH-induced assembly of PEG-SS-PDEA block copolymer, as shown in Figure S3A. Furthermore, ζ potential measurements revealed that protein-loaded PEG-SS-PDEA (9.2 k) polymersomes and PEG-PDEA (8.9 k) polymersomes had close to neutral surface charges (+2.4−3.5 mV) at pH 7.4 in 10 mM HEPES buffer (Table 2). In comparison, protein-loaded PEG-SS-PDEA (6.8 k) polymersomes displayed slightly higher positive surface charges (+5.6−7.7 mV) than the PEG-SS-PDEA (9.2 k) counterparts.

In the following, PEG-SS-PDEA (9.2 k) polymersomes due to their high protein loading and close to neutral surface charges were selected for further investigations. The protein release studies were carried out at 37 °C in four different media, i.e., PBS buffer (pH 7.4, 20 mM, 150 mM NaCl), PBS buffer with 10 mM DTT, acetate buffer (pH 6.0, 20 mM, 150 mM NaCl), and acetate buffer with 10 mM DTT. In line with our expectation, minimal protein (<20%) was released from FITC-BSA-loaded PEG-SS-PDEA (9.2 k) polymersomes as well as FITC-BSA-loaded PEG−PDEA (8.9 k) controls in 8 h at pH 7.4 and 37 °C (Figure 5A). The release of proteins was

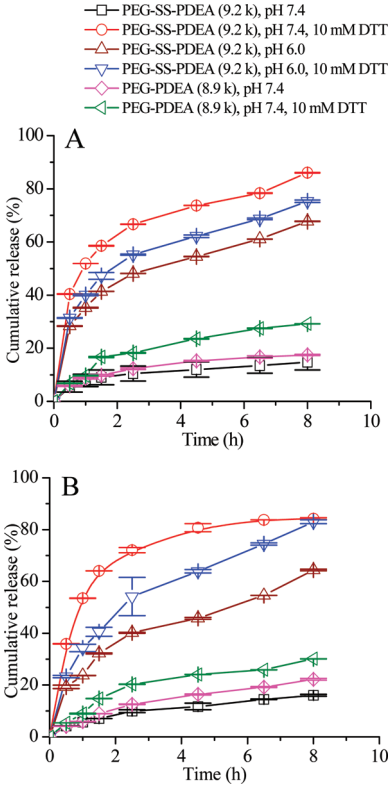

Figure 5. pH and/or reduction-triggered release of proteins from PEG-SS-PDEA (9.2 k) polymersomes. PEG-PDEA (8.9 k) polymersomes were used as a control. (A) Release of FITC-BSA; (B) release of FITC-CC.

significantly augmented at pH 6.0 due to protonation of PDEA, in which 67.7% FITC-BSA was released in 8 h under otherwise the same conditions (Figure 5A). The incomplete protein release is likely due to existing interactions between protein and PDEA block. As revealed by DLS, FITC-BSA-loaded polymersomes maintained a size of ca. 22 nm following an 8 h release at pH 6.0 (Figure S3B). Most strikingly, the fastest protein release was observed under intracellular-mimicking reductive environ-

dx.doi.org/10.1021/la203843m | Langmuir 2012, 28, 2056−2065

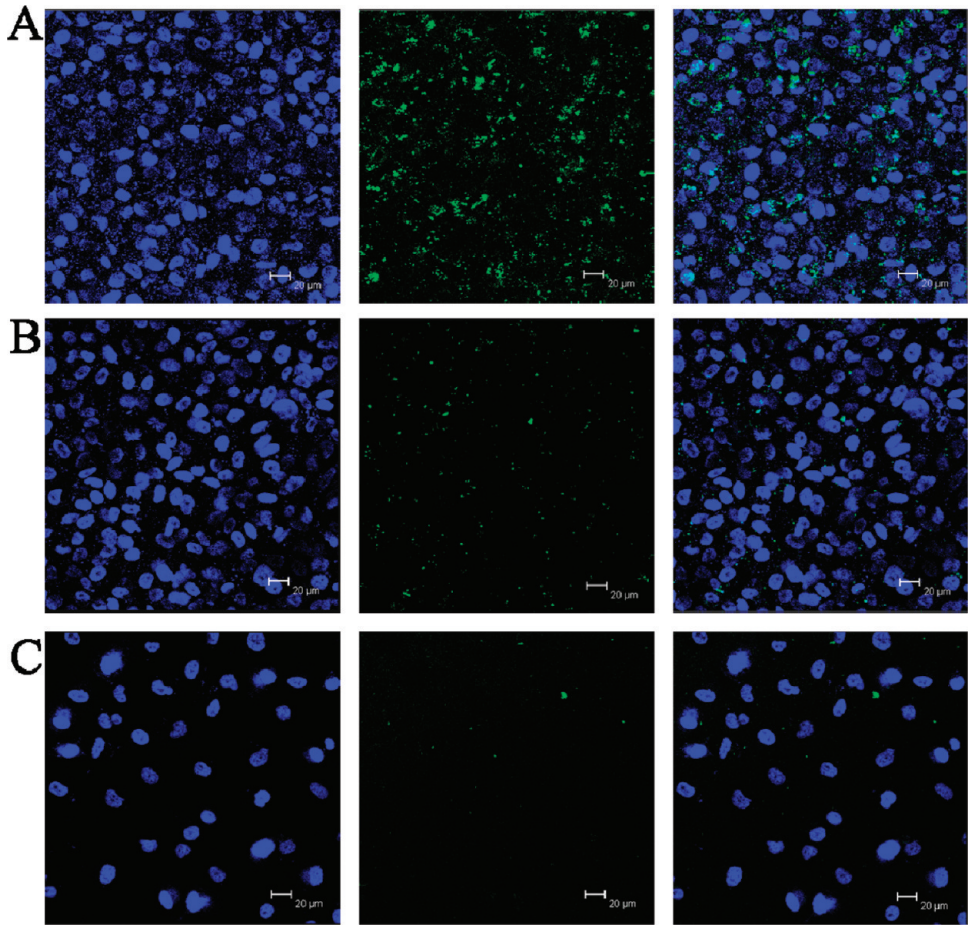

Figure 6. CLSM images of MCF-7 cells incubated for 6 h with FITC-CC-loaded PEG-SS-PDEA (9.2 k) polymersomes (A), FITC-CC-loaded reduction-insensitive PEG−PDEA (8.9 k) polymersomes (B), and free FITC-CC (C). FITC-CC concentration was set at 40 μg/mL. For each panel, images from left to right: nuclei stained by DAPI (blue), FITC-CC fluorescence (green), and overlays of two images. The scale bars represent 20 μm in all the images.

ments (10 mM DTT, pH 7.4), which resulted in 86.1% FITC-BSA release in 8 h (Figure 5A). It should be noted that protein release was not much enhanced by 10 mM DTT at pH 6.0 (Figure 5A), most probably due to inefficient reduction under acidic conditions. Similar release profiles were also observed for FITC-CC (Figure 5B). These results indicate that protein is released from protein-loaded PEG-SS-PDEA polymersomes in response to endosomal pH and cytoplasmic reducing conditions.

The cellular uptake and intracellular protein release behaviors of protein-loaded PEG-SS-PDEA (9.2 k) polymersomes were studied in MCF-7 cells using CLSM. Notably, strong FITC-CC fluorescence was observed in MCF-7 cells following 6 h of incubation with FITC-CC-loaded PEG-SS-PDEA (9.2 k) polymersomes (Figure 6A). In comparison, MCF-7 cells treated with FITC-CC-loaded PEG−PDEA (8.9 k) polymersomes (reduction-insensitive control) revealed much less FITC-CC fluorescence under otherwise the same conditions (Figure 6B), and practically no FITC-CC fluorescence was detected for cells incubated with free FITC-CC (Figure 6C). These results confirm that pH and reduction dual-bioresponsive polymersomes mediate efficient intracellular protein release. It is likely that the high buffer capacity of PDEA facilitates endosomal escape of protein-loaded polymersomes via the "proton sponge effect", while reductive cleavage of athe disulfide bond in the cytoplasm leads to efficient release of proteins.

Apoptotic Activity of CC-Loaded Dual-Bioresponsive Polymersomes. It is of utmost importance for protein carriers that released therapeutic proteins maintain their activity. MTT assays showed that PEG-SS-PDEA (9.2 k) polymersomes were practically nontoxic to both RAW 264.7 and MCF-7 cells (cell viability >85%) up to a tested concentration of 300 μg/mL (Figure 7). As shown above, preparation of protein-loaded polymersomes was performed under mild conditions, minimizing protein denaturation and/or inactivation. Herein, horse heart CC, which is known to play a significant role in programmed cell death,[46−48] was selected as a model therapeutic protein. The intracellularly injected CC was shown to induce effective cell apoptosis.[5,49,50] Recently, Perez et al. reported that intracellular CC delivery with nanoparticles caused appreciable apoptosis in MCF-7 cells.[51]

The apoptotic activity of CC-loaded PEG-SS-PDEA (9.2 k) polymersomes was studied in MCF-7 cells using flow cytometry. The level of apoptosis was determined by annexin V-FITC/PI staining. The results showed that CC-loaded PEG-SS-PDEA (9.2 k) polymersomes caused significant apoptosis of MCF-7 cells (42.9%) in 48 h at a CC dosage of 80 μg/mL (Figure 8A). By contrast, much lower levels of apoptosis were observed for CC-loaded reduction-insensitive PEG-PDEA (8.9 k) polymersomes (29.1%) and free CC (18.3%) under

dx.doi.org/10.1021/la203843m | *Langmuir* 2012, 28, 2056−2065

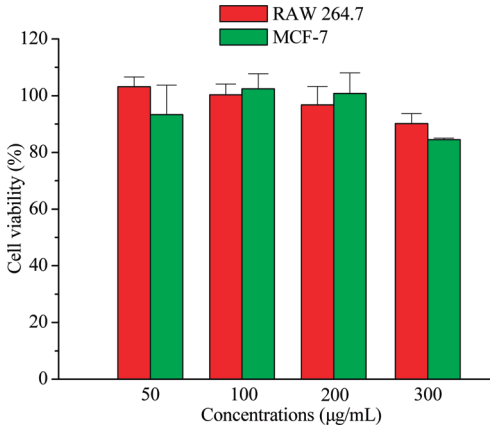

Figure 7. Cytotoxicity of PEG-SS-PDEA (9.2 k) polymersomes determined by MTT assays in RAW 264.7 and MCF-7 cells following 24 h of incubation (n = 4).

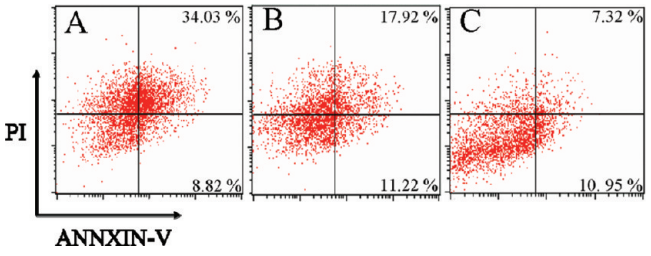

Figure 8. Contour diagram of Annexin V-FITC/PI flow cytometry of MCF-7 cells after 48 h of incubation with CC-loaded PEG-SS-PDEA (9.2 k) polymersomes (A), CC-loaded PEG-PDEA (8.9 k) polymersomes (B), and free CC (C). CC concentration was set at 80 μg/mL.

otherwise the same conditions (Figure 8B,C). These results corroborate that pH and reduction dual-bioresponsive PEG-SS-PDEA polymersomes are able to efficiently deliver and release CC into cancer cells, and, most importantly, released CC maintains its apoptotic activity.

CONCLUSIONS

We have demonstrated that pH and reduction dual-bioresponsive nanosized polymersomes based on PEG-SS-PDEA diblock copolymers are able to efficiently load and deliver CC into cancer cells, achieving superior anticancer activity. The proteins are loaded into polymersomes under mild conditions, minimizing protein denaturation and inactivation. These polymersomes are sufficiently stable with minimal protein release under physiological conditions (pH 7.4, 37 °C), while proteins are rapidly released in response to endosomal pH and/or intracellular-mimicking reductive environments. Importantly, intracellularly released proteins retain their biological activity. PEG-SS-PDEA copolymers are conveniently prepared by controlled RAFT polymerization. These pH and reduction dual-bioresponsive polymersomes are highly promising for targeted intracellular delivery of protein and peptide drugs.

ASSOCIATED CONTENT

Supporting Information

Calibration curves for FITC-BSA and FITC-CC, TEM characterization of polymersomes, polymersome size as a function of pH, as well as size distributions of FITC-BSA-loaded polymersomes following protein release at pH 6.0. This information is available free of charge via the Internet at http://pubs.acs.org/.

AUTHOR INFORMATION

Corresponding Author

*Tel/fax: +86-512-65880098. E-mail: zyzhong@suda.edu.cn.

ACKNOWLEDGMENTS

This work was supported by National Natural Science Foundation of China (NSFC 20874070, 50973078, 20974073, 51003070, and 51173126), a Project Funded by the Priority Academic Program Development of Jiangsu Higher Education Institutions, and the Program of Innovative Research Team of Soochow University.

REFERENCES

(1) Kerbel, R.; Folkman, J. *Nat. Rev. Cancer* **2002**, *2*, 727−739.
(2) Harries, M.; Smith, I. *Endocr.-Relat. Cancer* **2002**, *9*, 75−85.
(3) Schrama, D.; Reisfeld, R. A.; Becker, J. C. *Nat. Rev. Drug Discov.* **2006**, *5*, 147−159.
(4) Guo, B.; Zhai, D. Y.; Cabezas, E.; Welsh, K.; Nouraini, S.; Satterthwait, A. C.; Reed, J. C. *Nature* **2003**, *423*, 456−461.
(5) Zhivotovsky, B.; Orrenius, S.; Brustugun, O. T.; Doskeland, S. O. *Nature* **1998**, *391*, 449−450.
(6) Gu, Z.; Biswas, A.; Zhao, M.; Tang, Y. *Chem. Soc. Rev.* **2011**, *40*, 3638−3655.
(7) Crommelin, D. J. A.; Daemen, T.; Scherphof, G. L.; Vingerhoeds, M. H.; Heeremans, J. L. M.; Kluft, C.; Storm, G. *J. Controlled Release* **1997**, *46*, 165−175.
(8) Lee, Y.; Ishii, T.; Cabral, H.; Kim, H.; Seo, J.-H.; Nishiyama, N.; Oshima, H.; Osada, K.; Kataoka, K. *Angew. Chem., Int. Ed.* **2009**, *48*, 5309−5312.
(9) Van Tomme, S. R.; Hennink, W. E. *Expert Rev. Med. Dev.* **2007**, *4*, 147−164.
(10) Taluja, A.; Youn, Y. S.; Bae, Y. H. *J. Mater. Chem.* **2007**, *17*, 4002−4014.
(11) Yan, M.; Du, J. J.; Gu, Z.; Liang, M.; Hu, Y. F.; Zhang, W. J.; Priceman, S.; Wu, L. L.; Zhou, Z. H.; Liu, Z.; Segura, T.; Tang, Y.; Lu, Y. F. *Nat. Nanotechnol.* **2010**, *5*, 48−53.
(12) Christian, D. A.; Cai, S.; Bowen, D. M.; Kim, Y.; Pajerowski, J. D.; Discher, D. E. *Eur. J. Pharm. Biopharm.* **2009**, *71*, 463−474.
(13) LoPresti, C.; Lomas, H.; Massignani, M.; Smart, T.; Battaglia, G. *J. Mater. Chem.* **2009**, *19*, 3576−3590.
(14) Meng, F. H.; Zhong, Z. Y. *J. Phys. Chem. Lett.* **2011**, *2*, 1533−1539.
(15) Tanner, P.; Baumann, P.; Enea, R.; Onaca, O.; Palivan, C.; Meier, W. *Acc. Chem. Res.* **2011**, *44*, 1039−1049.
(16) Kishimura, A.; Koide, A.; Osada, K.; Yamasaki, Y.; Kataoka, K. *Angew. Chem., Int. Ed.* **2007**, *46*, 6085−6088.
(17) Kumar, M.; Grzelakowski, M.; Zilles, J.; Clark, M.; Meier, W. *Proc. Natl. Acad. Sci. U.S.A.* **2007**, *104*, 20719−20724.
(18) Rameez, S.; Alosta, H.; Palmer, A. F. *Bioconjugate Chem.* **2008**, *19*, 1025−1032.
(19) Demirgoz, D.; Pangburn, T. O.; Davis, K. P.; Lee, S.; Bates, F. S.; Kokkoli, E. *Soft Matter* **2009**, *5*, 2011−2019.
(20) Liu, G. J.; Ma, S. B.; Li, S. K.; Cheng, R.; Meng, F. H.; Liu, H. Y.; Zhong, Z. Y. *Biomaterials* **2010**, *31*, 7575−7585.
(21) Meng, F. H.; Zhong, Z. Y.; Feijen, J. *Biomacromolecules* **2009**, *10*, 197−209.
(22) Li, M. H.; Keller, P. *Soft Matter* **2009**, *5*, 927−937.
(23) Rapoport, N. *Prog. Polym. Sci.* **2007**, *32*, 962−990.
(24) Meng, F. H.; Hennink, W. E.; Zhong, Z. Y. *Biomaterials* **2009**, *30*, 2180−2198.
(25) Borchert, U.; Lipprandt, U.; Bilang, M.; Kimpfler, A.; Rank, A.; Peschka-Suss, R.; Schubert, R.; Lindner, P.; Forster, S. *Langmuir* **2006**, *22*, 5843−5847.

(26) Agut, W.; Brulet, A.; Schatz, C.; Taton, D.; Lecommandoux, S. *Langmuir* **2010**, *26*, 10546−10554.
(27) Holowka, E. P.; Sun, V. Z.; Kamei, D. T.; Deming, T. J. *Nat. Mater.* **2007**, *6*, 52−57.
(28) Du, J. Z.; Tang, Y. P.; Lewis, A. L.; Armes, S. P. *J. Am. Chem. Soc.* **2005**, *127*, 17982−17983.
(29) Lomas, H.; Canton, I.; MacNeil, S.; Du, J.; Armes, S. P.; Ryan, A. J.; Lewis, A. L.; Battaglia, G. *Adv. Mater.* **2007**, *19*, 4238−4243.
(30) Cerritelli, S.; Velluto, D.; Hubbell, J. A. *Biomacromolecules* **2007**, *8*, 1966−1972.
(31) Xu, H. F.; Meng, F. H.; Zhong, Z. Y. *J. Mater. Chem.* **2009**, *19*, 4183−4190.
(32) Xu, P. S.; Van Kirk, E. A.; Zhan, Y. H.; Murdoch, W. J.; Radosz, M.; Shen, Y. Q. *Angew. Chem., Int. Ed.* **2007**, *46*, 4999−5002.
(33) Thang, S. H.; Chong, Y. K.; Mayadunne, R. T. A.; Moad, G.; Rizzardo, E. *Tetrahedron Lett.* **1999**, *40*, 2435−2438.
(34) Zhu, C. H.; Jung, S. Y.; Luo, S. B.; Meng, F. H.; Zhu, X. L.; Park, T. G.; Zhong, Z. Y. *Biomaterials* **2010**, *31*, 2408−2416.
(35) Zhan, F. X.; Chen, W.; Wang, Z. J.; Lu, W. T.; Cheng, R.; Deng, C.; Meng, F. H.; Liu, H. Y.; Zhong, Z. Y. *Biomacromolecules* **2011**, *12*, 3612−3620.
(36) Jiang, X. Z.; Luo, S. Z.; Armes, S. P.; Shi, W. F.; Liu, S. Y. *Macromolecules* **2006**, *39*, 5987−5994.
(37) Du, J. Z.; Armes, S. P. *J. Am. Chem. Soc.* **2005**, *127*, 12800−12801.
(38) Yu, S.; Azzam, T.; Rouiller, I.; Eisenberg, A. *J. Am. Chem. Soc.* **2009**, *131*, 10557−10566.
(39) Meng, F. H.; Engbers, G. H. M.; Feijen, J. *J. Controlled Release* **2005**, *101*, 187−198.
(40) Adams, D. J.; Butler, M. F.; Weaver, A. C. *Langmuir* **2006**, *22*, 4534−4540.
(41) Sun, H. L.; Guo, B. N.; Cheng, R.; Meng, F. H.; Liu, H. Y.; Zhong, Z. Y. *Biomaterials* **2009**, *30*, 6358−6366.
(42) Sun, H. L.; Guo, B. N.; Li, X. Q.; Cheng, R.; Meng, F. H.; Liu, H. Y.; Zhong, Z. Y. *Biomacromolecules* **2010**, *11*, 848−854.
(43) Kirby, C.; Gregoriadis, G. *Nat. Biotechnol.* **1984**, *2*, 979−984.
(44) Lee, J. C. M.; Bermudez, H.; Discher, B. M.; Sheehan, M. A.; Won, Y. Y.; Bates, F. S.; Discher, D. E. *Biotechnol. Bioeng.* **2001**, *73*, 135−145.
(45) Arifin, D. R.; Palmer, A. F. *Biomacromolecules* **2005**, *6*, 2172−2181.
(46) Kim, R.; Tanabe, K.; Uchida, Y.; Emi, M.; Inoue, H.; Toge, T. *Cancer Chemother. Pharmacol.* **2002**, *50*, 343−352.
(47) Li, K.; Li, Y. C.; Shelton, J. M.; Richardson, J. A.; Spencer, E.; Chen, Z. J.; Wang, X. D.; Williams, R. S. *Cell* **2000**, *101*, 389−399.
(48) Liu, X. S.; Kim, C. N.; Yang, J.; Jemmerson, R.; Wang, X. D. *Cell* **1996**, *86*, 147−157.
(49) Ow, Y. L. P.; Green, D. R.; Hao, Z.; Mak, T. W. *Nat. Rev. Mol. Cell Biol.* **2008**, *9*, 532−542.
(50) Brustugun, O. T.; Fladmark, K. E.; Doskeland, S. O.; Orrenius, S.; Zhivotovsky, B. *Cell Death Differ.* **1998**, *5*, 660−668.
(51) Santra, S.; Kaittanis, C.; Perez, J. M. *Mol. Pharmaceutics* **2010**, *7*, 1209−1222.